REPORT DOCUMENTATION PAGE

Form Approved
OMB No. 0704-0188

Public reporting burden for this collection of information is estimated to average 1 hour per response, including the time for reviewing instructions, searching existing data sources, gathering and maintaining the data needed, and completing and reviewing this collection of information. Send comments regarding this burden estimate or any other aspect of this collection of information, including suggestions for reducing this burden to Department of Defense, Washington Headquarters Services, Directorate for Information Operations and Reports (0704-0188), 1215 Jefferson Davis Highway, Suite 1204, Arlington, VA 22202-4302. Respondents should be aware that notwithstanding any other provision of law, no person shall be subject to any penalty for failing to comply with a collection of information if it does not display a currently valid OMB control number. **PLEASE DO NOT RETURN YOUR FORM TO THE ABOVE ADDRESS.**

1. REPORT DATE (DD-MM-YYYY)	2. REPORT TYPE		3. DATES COVERED (From - To)
23-03-2007	Technical Paper and Briefing Charts		

4. TITLE AND SUBTITLE	5a. CONTRACT NUMBER
Code Validation of CFD Heat Transfer Models for Liquid Rocket Engine Combustion Devices	5b. GRANT NUMBER
	5c. PROGRAM ELEMENT NUMBER

6. AUTHOR(S)	5d. PROJECT NUMBER
E.B. Coy	50260548
	5e. TASK NUMBER
	5f. WORK UNIT NUMBER

7. PERFORMING ORGANIZATION NAME(S) AND ADDRESS(ES)	8. PERFORMING ORGANIZATION REPORT NUMBER
AFRL/PRSA 10 E. Saturn Blvd. Edwards AFB CA 93524-7680	AFRL-PR-ED-TP-2007-157

9. SPONSORING / MONITORING AGENCY NAME(S) AND ADDRESS(ES)	10. SPONSOR/MONITOR'S ACRONYM(S)
Air Force Research Laboratory (AFMC) AFRL/PRS 5 Pollux Drive Edwards AFB CA 93524-7048	11. SPONSOR/MONITOR'S NUMBER(S) AFRL-PR-ED-TP-2007-157

12. DISTRIBUTION / AVAILABILITY STATEMENT

Distribution A: Approved for public release; distribution unlimited. (Public Affairs No. 07120A).

13. SUPPLEMENTARY NOTES
Presented at the JANNAF 54th Propulsion Meeting/3rd Liquid Propulsion Subcommittee/2nd Spacecraft Propulsion Subcommittee/5th Modeling and Simulation Subcommittee Joint Meeting, Denver, CO, 14-17 May 2007.

14. ABSTRACT
This paper reports on the development of a new heat transfer test rig for exploratory testing of new technologies for controlling chamber wall heat transfer. The design of the rig and its capabilities are described. A second objective of the test rig is to provide CFD validation data under conditions relevant to liquid rocket engine thrust chambers. The approach to validation that was adopted was to establish the minimum level of validation uncertainty that can be achieved for a fully-reacted, uniform flow. A method for characterizing the surface temperature and heat flux to the wall is described based on sensors embedded within the wall of the chamber.

15. SUBJECT TERMS

16. SECURITY CLASSIFICATION OF:			17. LIMITATION OF ABSTRACT	18. NUMBER OF PAGES	19a. NAME OF RESPONSIBLE PERSON Dr. Edward B. Coy
a. REPORT	b. ABSTRACT	c. THIS PAGE	SAR	44	19b. TELEPHONE NUMBER (include area code) (661) 275-5219
Unclassified	**Unclassified**	**Unclassified**			

Standard Form 298 (Rev. 8-98)
Prescribed by ANSI Std. 239.18

CODE VALIDATION OF CFD HEAT TRANSFER MODELS FOR LIQUID ROCKET ENGINE COMBUSTION DEVICES (PREPRINT)

E.B. Coy
Air Force Research Laboratory
Edwards AFB, CA

ABSTRACT

This paper reports on the development of a new heat transfer test rig for exploratory testing of new technologies for controlling chamber wall heat transfer. The design of the rig and its capabilities are described. A second objective of the test rig is to provide CFD validation data under conditions relevant to liquid rocket engine thrust chambers. The approach to validation that was adopted was to establish the minimum level of validation uncertainty that can be achieved for a fully-reacted, uniform flow. A method for characterizing the surface temperature and heat flux to the wall is described based on sensors embedded within the wall of the chamber.

INTRODUCTION

The design of a liquid rocket engine combustion chamber involves tradeoffs that affect the wall temperature and the heat flux. Lowering the wall temperature can increase the engine life but generally reduces the performance. Lowered wall temperatures provide increased margin for hot-spots in the flow-field and increased strength of the wall material providing additional margin for stress; however methods used to lower wall temperature can reduce engine performance. Film cooling causes a fraction of the propellant to react at mixture ratios which are far from the optimum for achieving maximum specific impulse. Increasing the effectiveness of the cooling channels generally results in increased pumping losses and reduced chamber pressure.

Expander cycle engines utilize the heat transferred through the chamber wall to the fuel to provide the energy to drive the turbopump. The pressure delivered by the pump and the maximum achievable chamber pressure are limited by the amount of heat that can be transferred through the chamber wall. A straightforward way to increase the heat is by extending the length of the chamber; however, this approach adversely affects the thrust to weight ratio of the engine. It also results in longer cooling channels so some of the additional head delivered by the pump is expended as pressure loss in the cooling channels instead of increased chamber pressure.

The rate at which heat is transferred to the wall of the combustion chamber is controlled by the flow properties on the hot-gas side. This flow can be divided into a boundary layer region and an outer flow region. Phenomena that affect heat transfer across the boundary layer include the wall surface conditions, the pressure gradient imposed on the boundary layer, the presence or absence of transpiration flow, the level of turbulence in the outer flow, and the fluid thermal and transport properties. The focus of the current program is on these phenomena. The outer flow is influenced by a large number of phenomena related to the injection, mixing, and reaction of propellants and the resulting fluid conditions, velocities, levels of turbulence and pressure gradient that are imposed on the boundary layer. These phenomena are being addressed by another program within AFRL/PR and are outside the scope of the current effort.

Numerous innovative techniques for controlling chamber wall temperature and heat flux have been proposed that provide the desired benefits while minimizing the adverse consequences. Due to the critical need to minimize risk, few of these approaches have been transitioned to flight systems. Transitioning these technologies requires a complete understanding of their effects on engine metrics. Sub-scale tests and modeling and simulation studies are the primary methods for advancing this understanding and retiring risks.

Sub-scale testing of LRE chambers has traditionally been used for obtaining heat flux data associated with particular injector designs. This testing has been conducted using heat-sink, calorimetric and ablative chambers depending on the technical needs of the program and available budget.   This type of testing effectively mitigates risk at the full-scale, but is relatively expensive and is rarely used for exploring new design approaches.

There exists an unmet need for sub-scale testing that is directed towards evaluation and development of new approaches. AFRL has used sub-scale testing for evaluating design variations, for example, developing a ranking of the heat transfer enhancement effectiveness of riblets and grooves[1]. It has also been used for examining the effectiveness of several configurations of Lamilloy wall material for transpiration cooling[2]. This work can proceed from cold-flow, low-pressure facilities, through facilities of increasing realism, at each step selecting the most promising designs for evaluation at the next level. Sub-scale testing can be used to evaluate new chamber and nozzle materials by subjecting them to reacting propellants at representative pressures and heat flux levels. Test coupons can be subjected to hundreds of thermal cycles relatively inexpensively in a sub-scale facility.

Sub-scale testing can be used for validation of analytical models, retiring the risks associated with the use of those models in engine design. Establishing the credibility of modeling and simulation tools at the sub-scale level where high-fidelity measurements can be performed is a critical step in gaining acceptance for the use of these tools and realizing the benefits of reduced design cycle times and costs.

The Air Force Research Laboratory, Propulsion Directorate, has developed a new heat transfer test rig specifically for the purpose of providing a flexible test bed for evaluating new control strategies for chamber wall temperature and heat flux, and also to provide data appropriate for model validation purposes. This paper documents the design of the test rig and its capabilities. This paper also describes a method that has been developed for measuring the wall temperature and heat flux.

TECHNICAL APPROACH

A literature review was performed to gather information on heat flux test rigs to determine the state of the art, and identify best practices and unmet needs. This review included laboratory wind-tunnels and flow loops, as well as sub-scale rocket devices. The literature review identified twenty four reports that contained discussions of heat flux tests on sub-scale rocket chambers and of these, twelve contained data. Nine sets were from experiments and three sets from CFD calculations. Of the experimental data, three data sets were based on hydrocarbon fuel and six sets were based on hydrogen: two data sets from DASA/Benz group, three sets from NASA and two sets from Penn State. Of these data sets, only the data produced by Penn State was intended for comparison with CFD predictions. However, all of the published data sets lack careful estimates of measurement uncertainty. The review makes clear that code validation for rocket combustion chamber conditions is in its infancy.

The results of the literature review were combined with lessons-learned from an earlier-design heat flux rig in our laboratory in creating design requirements for the new rig. The top-level technical requirements can be summarized as:

1. Adaptable to studies of transpiration cooling, film cooling, heat transfer enhancement, and material durability, with gaseous and liquid fuels
2. Ability to insert samples of chamber wall materials as interchangeable "coupons"
3. Well-mixed, fully-reacted, uniform-velocity inlet flow to the test section
4. Ability to control flow velocity over the coupon
5. Highly reliable and accurate measurements of wall temperature and heat flux
6. Optical accessibility for line-of-sight transmission-measurements in the boundary layer that is minimally invasive to flow
7. Optical accessibility for flow-field and chamber wall imaging
8. Operate with conventional rocket propellants at conditions relevant to AF programs
9. Scaled to operate in the AFRL/PRSA EC-1 facility

A cutaway view of the new heat flux rig is shown in figure 1. The injector for gaseous hydrogen and oxygen consists of 25 coaxial elements arranged in a square pattern. The propellants pass through a distribution plate containing 16 holes that are staggered relative to the oxygen posts. Each oxygen post contains precision orifice a 0.89 +/- .0076 mm (0.035 +/-.0003 inch) pressed into the inlet to balance the flow. The alignment of the oxygen posts within the

hydrogen annuli is maintained by a plate that is fit into the backside of the injector faceplate. The exits of the oxygen posts are recessed half a diameter from the surface of the faceplate. The hydrogen enters the injector at four locations spaced evenly around the periphery of a manifold. The hydrogen passes through sixteen holes in the oxygen post alignment plate which also serves as a distribution plate for the hydrogen. The hydrogen impinges on the backside of the injector faceplate and then passes through the annuli formed between the oxygen posts and the holes in the injector faceplate. The injector parts were sized to produce an oxygen injection velocity of 40 m/s (130 ft/s) and a hydrogen velocity of 200 m/s (650 ft/s) assuming a chamber contraction ratio from the heat transfer section to the nozzle of 3. Water flow tests were performed to determine the uniformity of the flow. The average flow rate from each oxygen post and hydrogen annulus was measured individually at a Reynolds number that matched the rated flow condition. The variability of the oxygen flow rates was +/- 1.5% (1 standard deviation) and the hydrogen was +/- 3%. The injector has operated successfully in hot-fire at chamber pressures up to 4.8 MPa (700 psi).

The propellants are injected into a 5.08 cm (2 inch) square chamber that is 7.6 cm (3 inch) in length. The flow then passes through a contraction before entering the 2.54 cm square heat transfer test section. The volume upstream of the entrance to the heat transfer section corresponds to an L* value of 1.3 m (51 inch) for a 3:1 contraction ratio nozzle. The volume and residence time should be adequate to ensure a completely reacted flow at the entrance of the heat transfer section. The contraction section will contribute to a uniform, relatively flat, inlet velocity profile. This relatively simple and well-controlled flow eliminates many of the complexities associated with the flow outside the boundary layer in keeping with the stated objective of this program of focusing on the boundary layer phenomena. This section also contains the engine igniter which is a hydrogen-oxygen torch.

The cross-section of the measurement section is square or rectangular. This facilitates testing of chamber wall designs as they can be inserted as coupons into the top or bottom of the channel. The fabrication of small rectangular coupons is always much simpler and less costly than fabrication of an entire sub-scale chamber. The test coupons are 15.24 cm (6 inch) long by 2.54 cm (1 inch) wide. The flat sides of the channel also facilitate the use of optical diagnostics for gas conditions. There are two sets of windows. The smaller windows are intended to function as narrow slits in the wall of the chamber that are minimally invasive. The windows are 9.5 mm (.375 inch) high by 3.2 mm (.125 inch) wide and can be purged with inert gas. These windows were designed for use with transmission diagnostics. The second set of windows are 2.54 cm (1 inch) high by 1.27 cm (½ inch) wide and were intended to allow radiometric temperature measurements of wall temperature and limited amounts of flow visualization to establish the uniformity of the flow in the test section. These windows can also be purged with inert gas. Finally, the top or bottom wall can be replaced with a contoured wall to produce an accelerating flow, a step change in cross-section, or a converging-diverging nozzle.

A set of nozzles is available for varying contraction ratio but it is typically in the range of 3. At a contraction ratio of 3, flow rate limitations of the facility set the upper limit on chamber pressure at approximately 5 MPa (750 psi). The heat flux at this pressure will be in the range of 40 MW/m^2 (25 Btu/in^2/s). The flow velocity can be controlled by changing the exit nozzle diameter; however, if the contraction ratio is increased too far the exit velocities of the injector will be too low allowing a flame to anchor at the injector and damaging the injector.

Heat transfer studies require accurate characterization of both the wall and the fluid conditions. The wall measurements required are the temperature, heat flux and the surface configuration, such as the roughness height, or riblet dimensions. The gas measurements are the pressure, temperature, species concentrations, velocity profiles and turbulence statistics. The following section discusses the methods being used to characterize the wall conditions. Methods used to characterize gas-side conditions will be the subject of future reports.
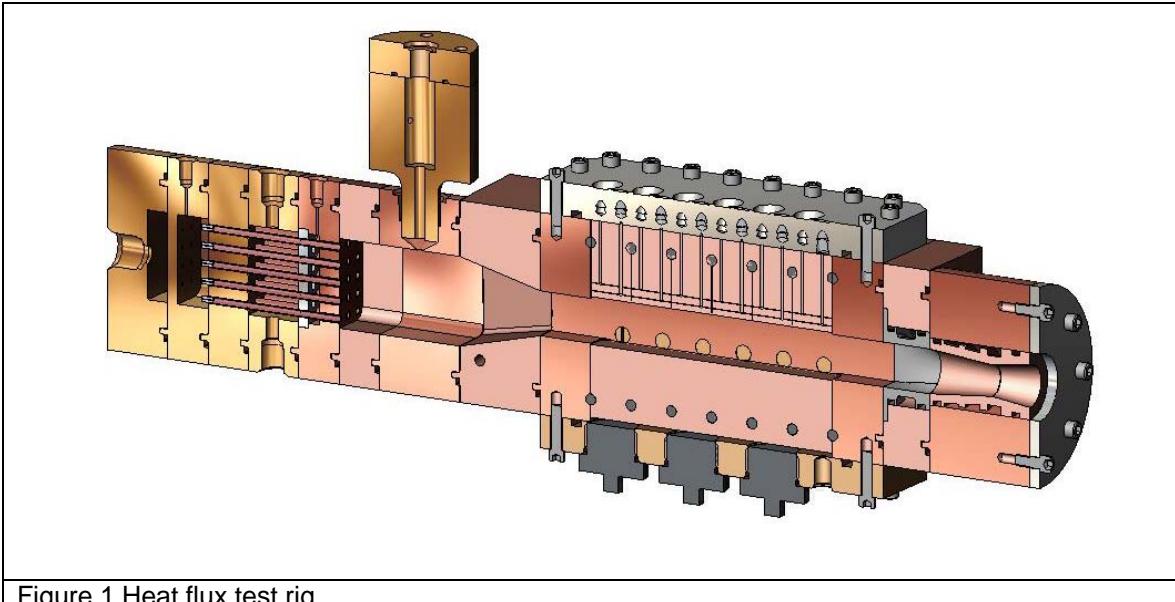
Figure 1 Heat flux test rig

WALL CONDITIONS

The following section describes the work that was performed to develop a robust method for accurate measurement of the wall conditions. It is currently not possible to calibrate heat flux sensors at levels of heat flux relevant to rocket combustion chambers, therefore the measurement must rely on an accurate physical model of the transducer and a record of as-built dimensions. Uncertainty estimates must be based on a first principles approach using the propagation of error methodology. Likewise, the transducer must be designed to conform as nearly as possible to the physical model. In the design of the heat flux rig, the sensor, the physical model and the data reduction algorithm were developed in concert. The following section describes the products of this effort.

The basic requirements for the transducer were:

1. operate at heat flux levels up to 50 MW/m^2 (30 Btu/in^2/s)
2. compatible with combustion products
3. can be inserted into a copper wall without disturbing the temperature or heat flux
4. response time of 0.1 seconds
5. can measure heat flux to a wall with heat transfer enhancement features such as riblets or dimples
6. convenient to install and operate

Surface junction thermocouples came closest to satisfying these requirements; however, they are prone to failure. Repair is possible but requires disassembly of the test article. For best results, surface junction thermocouples must be installed by the manufacturer. The drawbacks of surface junction thermocouples are that they are not compatible with walls with surface features and they produce noisy signals which must be filtered and this reduces the otherwise excellent time response.

Other types of transducer were also considered. Gardon gauges cannot be used for non-smooth surfaces because the gauge surface cannot be modified or the measurement response will be changed. Thermopiles and thin-film sensors do not meet the heat flux and temperature requirements. Infrared thermography is a technique that could potentially be adapted for use but needs development and testing under the test conditions before it can be applied.

Previous experience in our lab with embedded thermocouples showed that they were not prone to failure and produced a quiet signal. Furthermore, the surface could be modified for heat

transfer enhancement without disturbing the sensors. However a general method for accurately determining surface conditions based on embedded measurements was lacking.
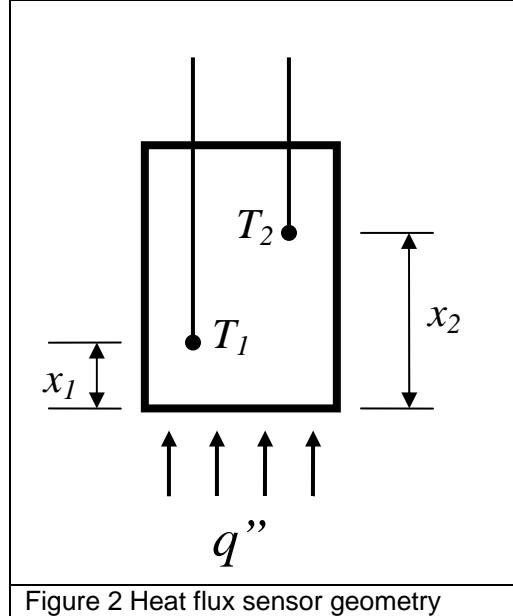
Figure 2 Heat flux sensor geometry

The goal of the following analysis is to obtain an expression for the heat flux and temperature at the surface, x=0, using temperatures measured at two depths within the block (see figure 1). The temperature profile in the block will be approximated using a cubic polynomial in x with time dependent coefficients.

$$T_i = a + bx_i + cx_i^2 + dx_i^3 \tag{1}$$

The four coefficients can be expressed in terms of the temperatures and rates of change of temperatures at the two interior points. An expression relating the time derivatives to the polynomial can be obtained by substituting into the heat conduction equation,

$$\frac{\partial T}{\partial t} = \alpha \frac{\partial^2 T}{\partial x^2} \tag{2}$$

$$\dot{T}_i = \alpha_i (2c + 6d\, x_i) \tag{3}$$

The system of equations relating the four coefficients to the four measurements can be written in matrix form,

$$\begin{bmatrix} 1 & x_1 & x_1^2 & x_1^3 \\ 1 & x_2 & x_2^2 & x_2^3 \\ 0 & 0 & 2\alpha_1 & 6\alpha_1 x_1 \\ 0 & 0 & 2\alpha_2 & 6\alpha_2 x_2 \end{bmatrix} \begin{bmatrix} a \\ b \\ c \\ d \end{bmatrix} = \begin{bmatrix} T_1 \\ T_2 \\ \dot{T}_1 \\ \dot{T}_2 \end{bmatrix} \tag{4}$$

The solution for the coefficients is,

$$d = \frac{\dfrac{\dot{T_2}}{\alpha_2} - \dfrac{\dot{T_1}}{\alpha_1}}{6(x_2 - x_1)} \tag{5}$$

$$c = \frac{\dfrac{\dot{T_2}}{\alpha_2} x_1 - \dfrac{\dot{T_1}}{\alpha_1} x_2}{2(x_1 - x_2)} \tag{6}$$

$$b = \frac{T_2 - T_1}{x_2 - x_1} - c \frac{x_2^2 - x_1^2}{x_2 - x_1} - d \frac{x_2^3 - x_1^3}{x_2 - x_1} \tag{7}$$

$$a = T_1 - b\, x_1 - c\, x_1^2 - d\, x_1^3 \tag{8}$$

The heat flux is obtained from Fourier's law,

$$q = -k \frac{\partial T}{\partial x} \tag{9}$$

$$q = -k\,(\, b + 2c\, x + 3d\, x^2\,) \tag{10}$$

At the surface (assumed to be $x=0$), the temperature and heat flux expressions are the following,

$$T_0 = a \tag{11}$$

$$q_0 = -k(T_0)\, b \tag{12}$$

Similar expressions can be derived for axi-symmetric heat flux in cylindrical coordinates or radially symmetric heat flux in spherical coordinates.

In principle, the two sensors can be placed anywhere within the wall, and there is no limitation on wall thickness. For example, the first sensor can be placed on the frontside surface, and the second sensor on the backside. However, the location of the sensors affects the frequency response as shown in the following section.

If the properties of the material are held constant, the sensor and model can be treated as an element in a linear control system. A finite-difference model was used to generate temperature data at interior points produced by a sinusoidally oscillating heat flux imposed on the x=0 surface. A typical result is given in figure 3. The model reproduces the input heat flux with a small change in amplitude and a phase lag. A relatively high frequency case (100 Hz) is shown to exaggerate the differences. This type of calculation was repeated for a number of frequencies and a Bode plot was constructed. The plotted frequency is the reciprocal of the non-dimensional Fourier number defined as,

$$Fo = \frac{\alpha}{x^2 f} \tag{13}$$

There are three relevant Fourier numbers in the problem, for the three dimensions, x_1, x_2 and l, the overall thickness of the slab, thus to completely describe the response would require a three dimensional space. However, a few preliminary calculations showed that for a given value of Fo_1, the optimum value of Fo_2 is approximately $10 Fo_1$ and that Fo_l does not have a significant effect.

The Bode plot given in figure 4 shows that the amplitude and phase are reproduced correctly for $1/Fo_1 <1$. If the base material is pure copper and a frequency response of 10 Hz is desired, then $x_1 < 3.4$ mm. Dimensions of this scale can be produced with a relative error of less than 1% using conventional machine shop technology.


Figure 3 Response of heat flux transducer and data reduction algorithm to sinusoidally oscillating heat flux.

Figure 4 Heat flux amplitude and phase response. Assumes constant thermal diffusivity (linear system) and $x_2/x_1=3$.
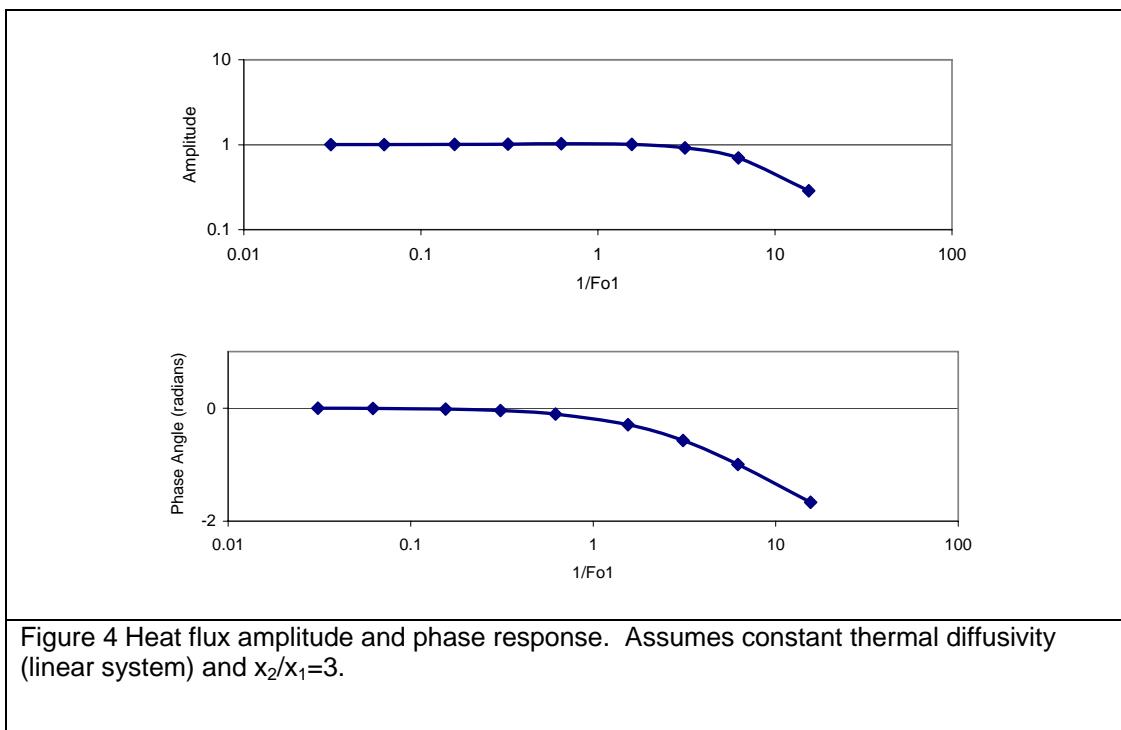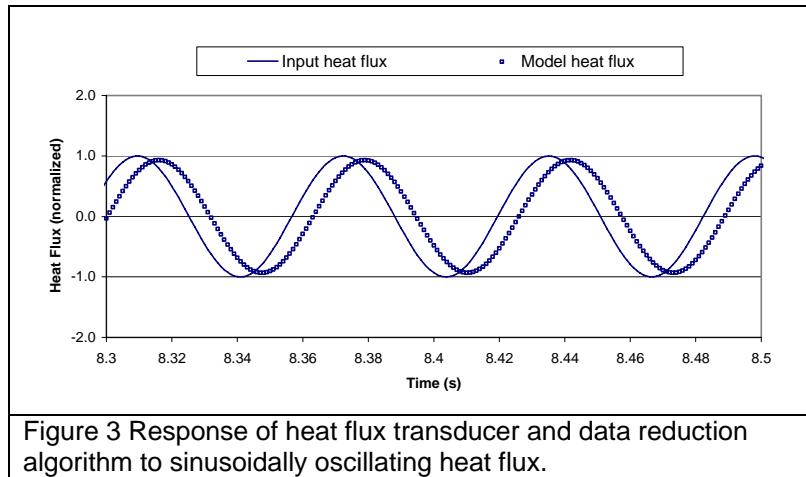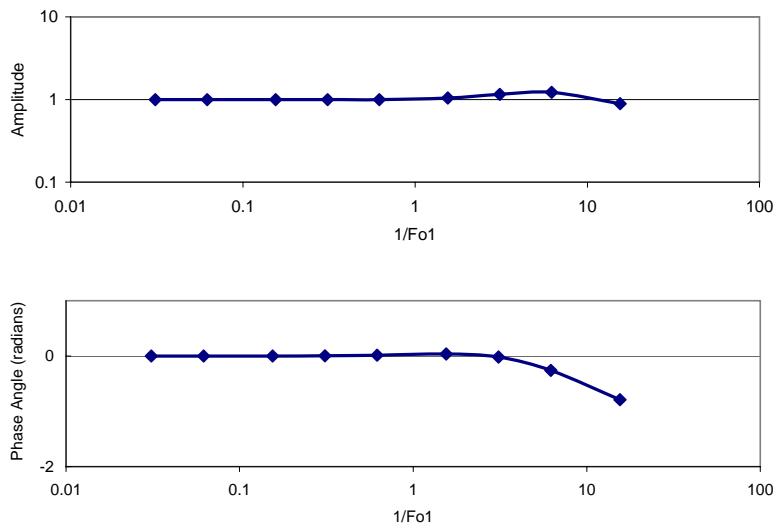
Figure 5 Surface temperature amplitude and phase response. Assumes constant thermal diffusivity (linear system) and $x_2/x_1=3$.

If the thermal properties are temperature dependent the system becomes non-linear. The effect of non-linearity increases with heat flux because the differences in temperature between the surface and the interior points are increased. The response of the transducer to a step change in heat flux to the highest expected value (3e7 W/m2) was modeled using the MatLab non-linear PDE solver, pdepe. This is a challenging problem for the sensor and algorithm because the step function contains high frequencies. The plot of transient temperatures shows the calculated temperatures at the surface and the two embedded sensor locations and the prediction of the polynomial model. The model results obscure the surface temperatures obtained with MatLab so a second plot is included that shows just the difference between the MatLab result and the polynomial model. After 0.1 seconds the polynomial model has converged to within 0.1 K.

Figure 6 Effects of temperature dependent properties on accuracy of surface temperature. Case is a step change in heat flux from 0-3e7 W/m^2. Model converges to within 0.1 K after 0.1 seconds. Material is copper.
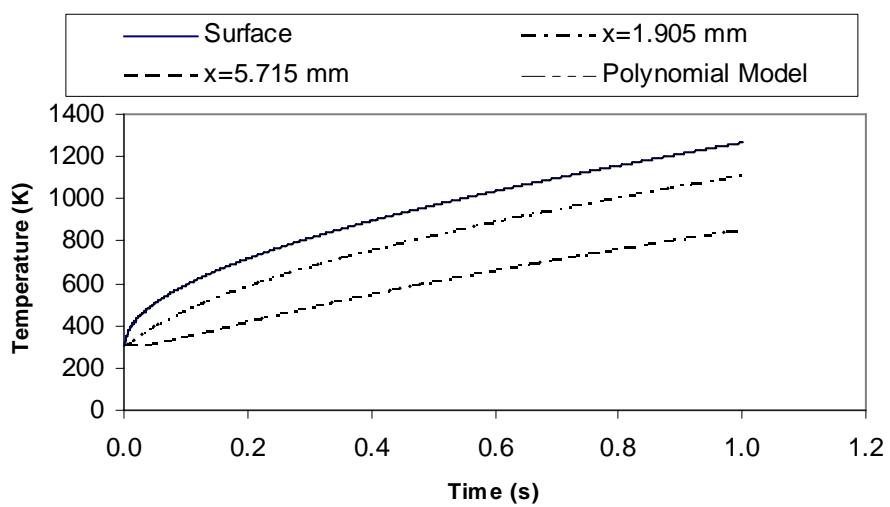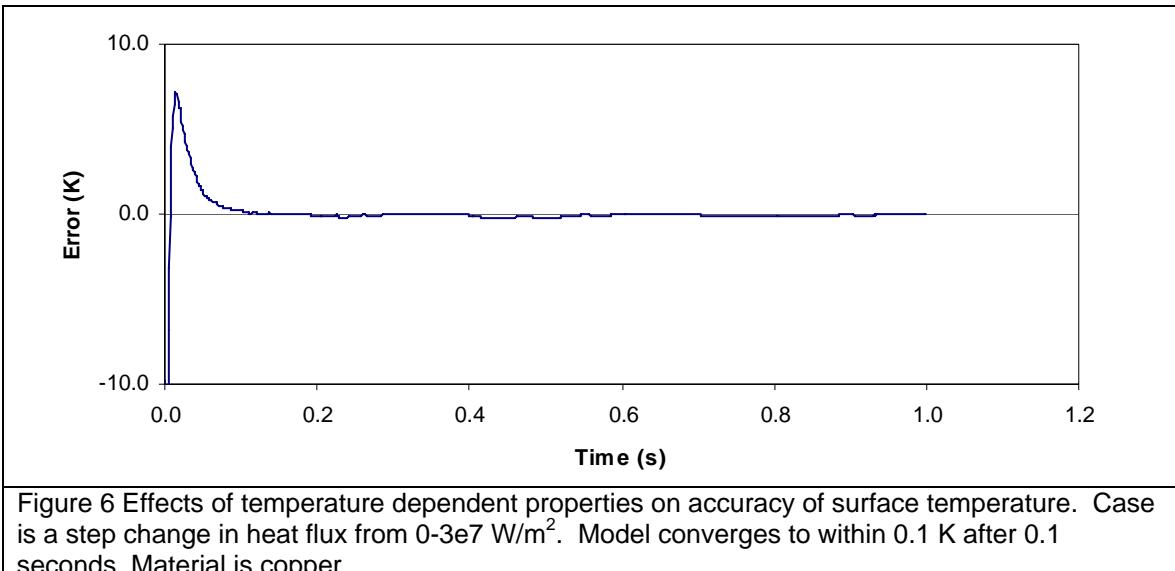
The performance of the polynomial model for heat flux is shown in the following figure. The model converges to the correct value within 0.1 seconds and the second plot shows the error is less than 0.1% after 0.1 seconds. In actual applications the overshoot behavior should not occur because the heat flux in an engine does not contain the high-frequency content of the step function.
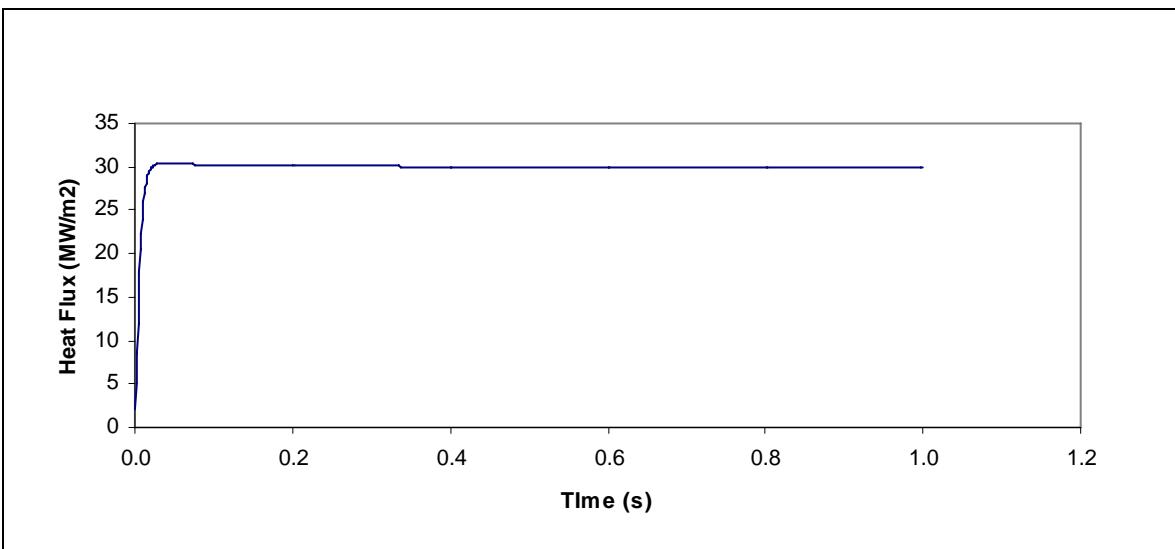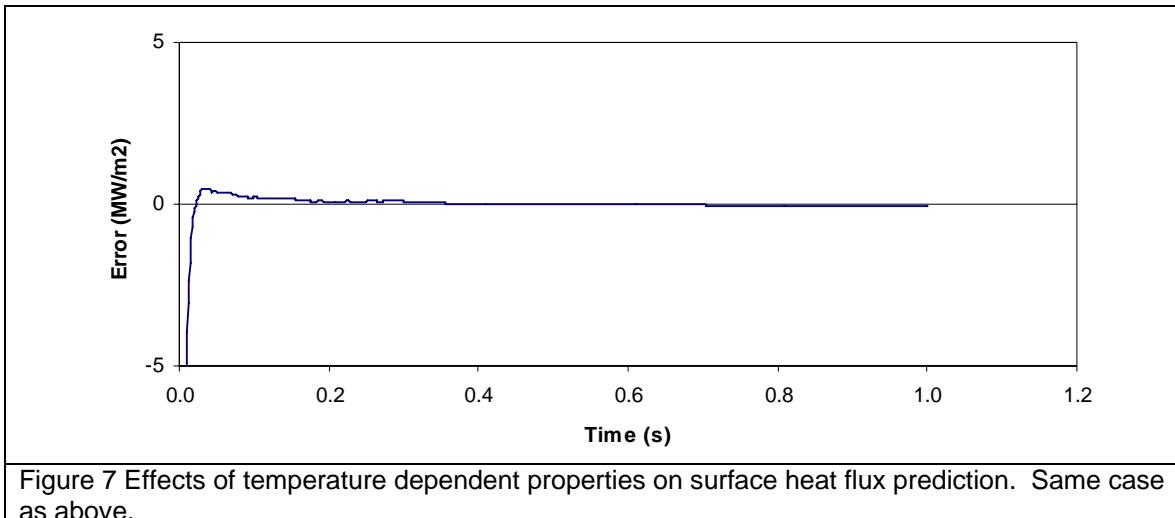
Figure 7 Effects of temperature dependent properties on surface heat flux prediction. Same case as above.

The above calculations show that the algorithm will not be a limiting factor in the accuracy of the heat flux measurement. The factors that will limit accuracy will be related to how closely the actual sensor conforms to the assumptions of the model. A new sensor design was required. The block that is to be instrumented is fabricated in two halves and grooves are cut in the mating surfaces to accommodate thermocouples. Conventional 0.063 inch thermocouple cable with stainless steel sheathing is stripped to expose the wires and these are placed into grooves that run parallel to the heat flux surface. The halves are mated and brazed and then the final machining of the heat transfer surface is performed.

The presence of the stainless steel sheathed thermocouples embedded in the copper base material will distort the flow of heat around the temperature measurement points and create errors relative to the model. To examine this effect a three dimensional numerical model of the sensor was created. The thermocouples were modeled as holes with adiabatic surfaces to maximize the effect and provide a conservative estimate of the error. Some plots of temperature are given in figure 8 showing the progress of the temperature wave with time. Distortions in the isotherms near the rounded ends of the thermocouple wells are visible. The temperature history at the thermocouple sensor locations was used as an input to the polynomial model and the results are given in figure 9. In this case the distortion in the temperature field caused by the thermocouples results in an error in the heat flux of approximately 2%. If necessary, this error could be reduced using a smaller diameter thermocouple or a thermocouple made from thin foil.
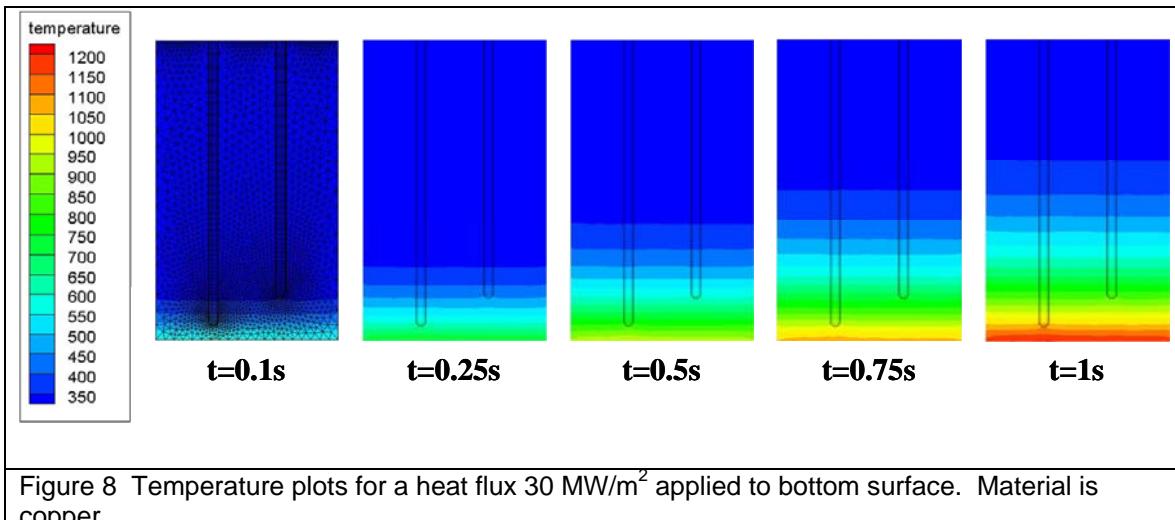

Figure 8 Temperature plots for a heat flux 30 MW/m^2 applied to bottom surface. Material is copper.
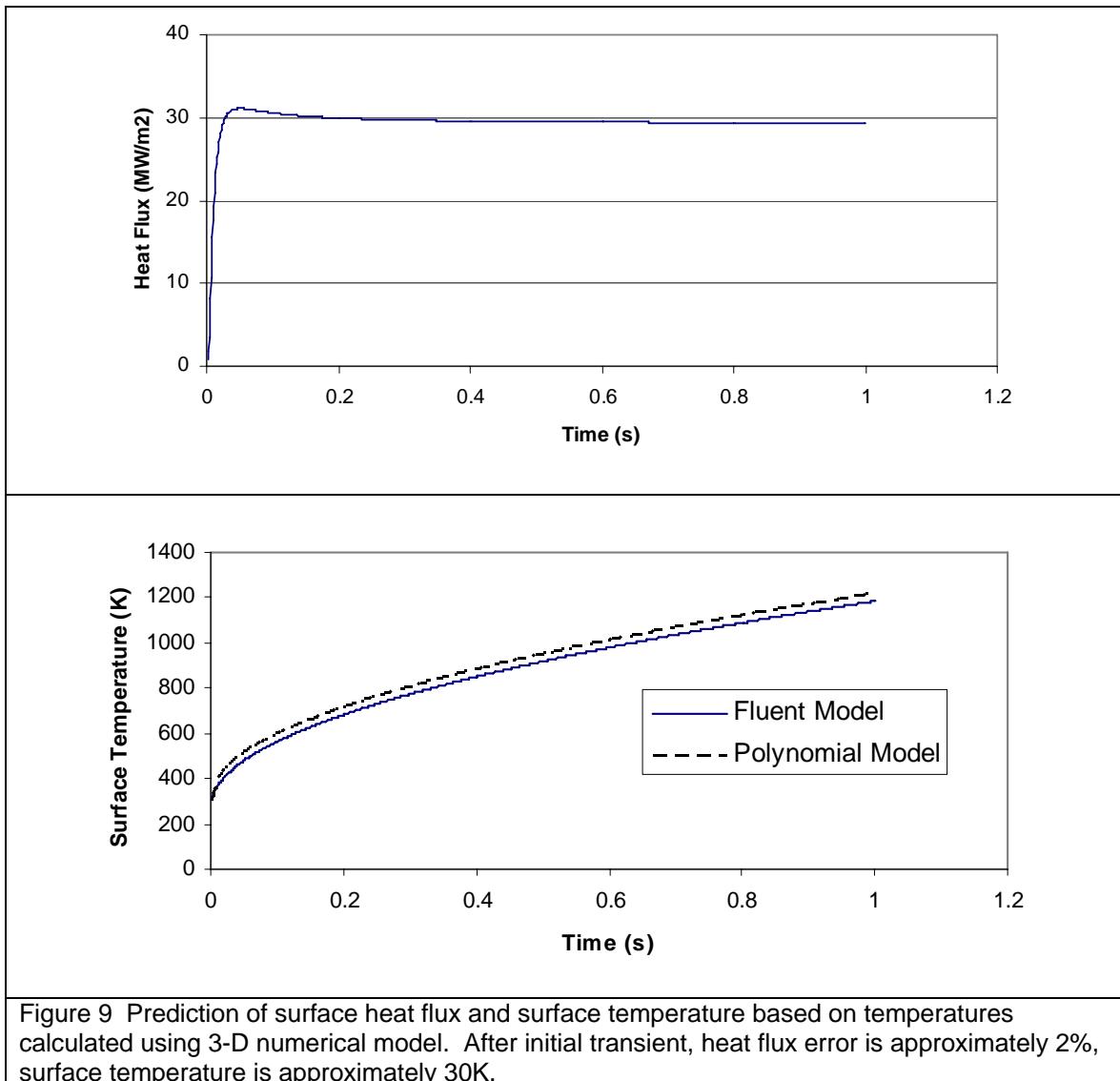
Figure 9 Prediction of surface heat flux and surface temperature based on temperatures calculated using 3-D numerical model. After initial transient, heat flux error is approximately 2%, surface temperature is approximately 30K.

CONCLUSIONS

The new heat transfer test rig is operational. It has been designed to produce a uniform inlet flow to facilitate accurate comparisons between various heat flux control schemes and to serve as a source of CFD validation data. In this paper the method that will be used for reporting surface temperatures and heat fluxes has been described. The method utilizes two temperature sensors embedded in the wall of the chamber. This method has the advantages of not requiring surface junction thermocouples which are prone to failure and produce noisy signals in rocket engine flows and is well suited for studies of the effects of surface features on heat transfer enhancement.   The method has been verified against analytical and numerical solutions and shown to not be a limiting factor with respect to accuracy or time response for representative conditions. A method for embedding sensors at precise depths within a wall has been described.

REFERENCES

[1] Coy, E.B., Danczyk, S., Watts, J., Poylio, J., Enhancement of Chamber Wall Heat Transfer by Surface Contouring, 53rd JPM/LPS, Monterrey, CA, Dec. 2006

[2] S.A. Danczyk, R. Cohn, E. Coy, T.P. Auyeung, Papesh, C., Sweeney, C., Experimental and Numerical Analysis of Transpiration Cooling of a Rocket Engine Using Lamilloy® Plates, 53rd JPM/LPS, Monterrey, CA, Dec. 2006

CODE VALIDATION OF CFD HEAT TRANSFER MODELS FOR LRE COMBUSTION DEVICES

Edward Coy

Propulsion Research Engineer

Propulsion Directorate

Air Force Research Laboratory

Outline

- **Significance of sub-scale testing for chamber wall heat transfer**

  – **Evaluation of heat transfer control methods**

  – **Model validation**

- **Heat flux rig**

  – **Lessons learned from previous work**

  – **New design**

  – **Robust, accurate method for wall temperature and heat flux**

Background
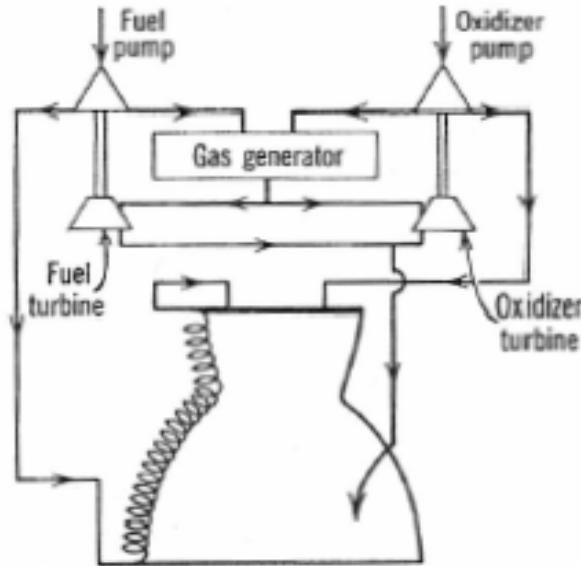
Gas Generator Cycle

- Boost engines

- Chamber pressure: 750-3000 psi

- Heat transfer technical challenge is preventing liner failure while minimizing impact on performance
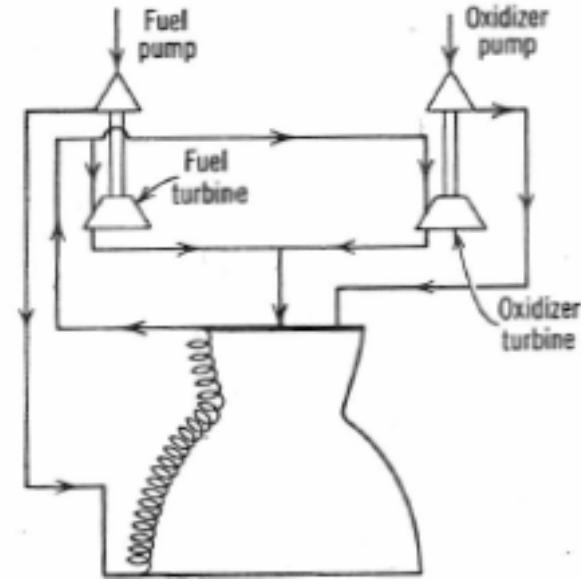
Expander Cycle

- Upper stage engines

- Chamber pressure: 250-1500 psi

- Heat transfer technical challenge is extracting sufficient heat from chamber to drive turbines without incurring large ΔP or long, heavy chamber

Background/SOA

- **SOA in for CFD Wall Heat Transfer Prediction is +/- 50%**

- **Engine programs continue to rely on subscale test data to predict full scale heat transfer**
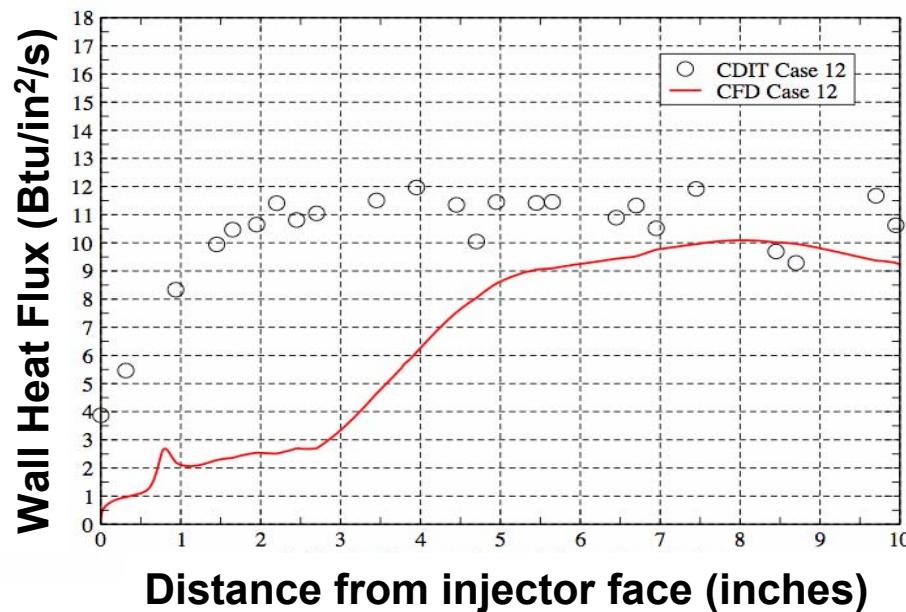
Blanching and cracking of SSME Chamber Liner

Legend:
- ○ CDIT Case 12
- — CFD Case 12

Wall Heat Flux (Btu/in^2/s) vs **Distance from injector face (inches)**

Typical comparison of CFD and test data from recent PSU/NASA CDIT Study

Significance

- **Inaccurate predictions can have major consequences**

  - **A 10% over estimate in heat transfer will require a 27% decrease in chamber pressure (Popp, 1994)**

  - **A 5% underestimate in heat transfer can reduce creep lifetime by 50% (Popp, 1994)**

  - **The most sensitive parameter in the engine power balance is the hot gas wall heat transfer coefficient (5X more sensitive than cooling channel HT, Johnson, 2005)**

- **Chamber life is controlled by hot-gas side wall temperature (800-1000 K)**

  - **Low cycle fatigue, thermal ratcheting**

Stress
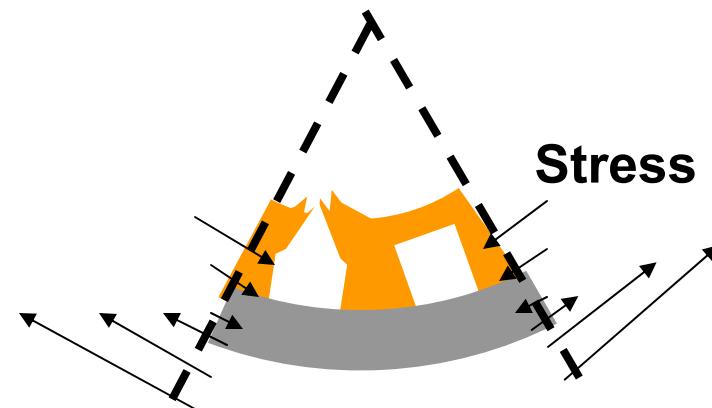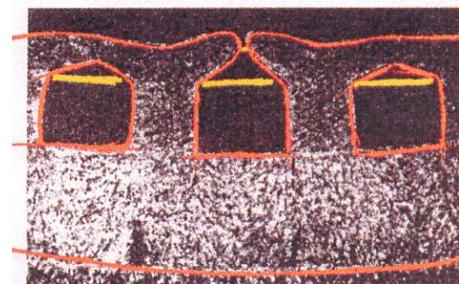
Heat Transfer Prediction

- **Why is prediction of heat transfer for rocket chamber conditions challenging?**

  - Requires accurate model of combustion processes to predict engine core flow

    - Injector flow, atomization, vaporization, mixing, turbulent combustion, secondary flows and recirculation zones

    - Contributes +/- 50 % to heat transfer uncertainty

  - Several boundary layer phenomena influence heat transfer

    - Wall roughness, free-stream turbulence, acoustic fluctuations, variable properties, severely cooled walls, rapid acceleration of outer flow, uncertain virtual origin of boundary layer, azimuthal curvature effects

    - Contributes +/- 20 % to heat transfer uncertainty

Previous Work at AFRL/PRSA on Chamber Wall Heat Transfer

- USET requires (1) predict and (2) maximize heat transfer in a high-performing expander cycle upper stage engine

  - Identified by USET contractors as a critical thrust chamber priority

- Increased heat transfer coefficient can reduce chamber length, weight, and cooling channel pressure drop. AFRL/NGST examined various wall contour options in PRSA EC-1 facility

  - GRCop-84 (Cu-8%Cr-4%Nb) high strength replacement for NARloy-Z

  - Fabricated by ASB Industries using cold-spray technique
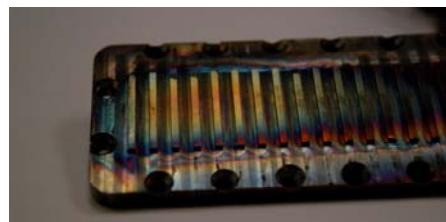
| Axial Ribs | Transverse Ribs | Transverse Grooves | Rough |
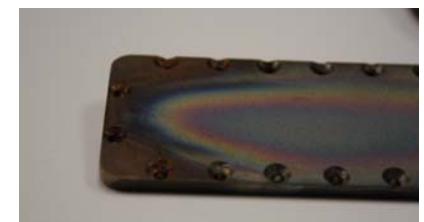
Transpiration Cooling For TR-107

- Evaluate Lamilloy for transpiration cooling for booster-class engines through hot-fire test in relevant environment.

- **Lamilloy ®** provides high levels of cooling effectiveness through a combination of:

  - High internal effectiveness (convection within tortuous passages)

  - Film cooling prevents heat transfer to metal surface

  - Conduction to internal areas where convection is high)
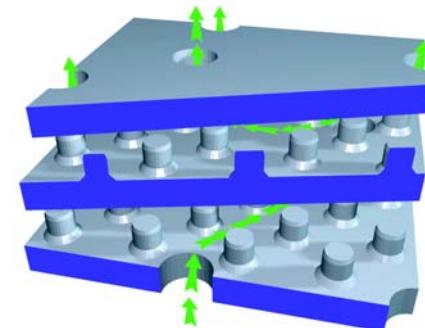

Cutaway showing tortuous passages

Post test view

Design Requirements for New Rig

- **Adaptable to studies of transpiration cooling, film cooling, heat transfer enhancement, and material durability, with gaseous and liquid fuels**

- **Ability to insert samples of chamber wall materials as interchangeable "coupons"**

- **Well-mixed, fully-reacted, uniform-velocity inlet flow to the test section**

- **Ability to control flow velocity over the coupon**

- **Highly reliable and accurate measurements of wall temperature and heat flux**

- **Optical accessibility for line-of-sight transmission-measurements in the boundary layer that is minimally invasive to flow**

- **Optical accessibility for flow-field and chamber wall imaging**

- **Operate with conventional rocket propellants at conditions relevant to AF programs**

- **Scaled to operate in the AFRL/PRSA EC-1 facility**

Heat Flux Rig

GOX Post Alignment Plate / GH_2 Distribution Plate

GOX/GH_2 Torch Igniter

GOX Manifold

Heat Flux Sensors

GOX Distribution Plate

Water cooled nozzle

GOX Orifices

GOX Posts

GH_2 Manifold

2"-1" Contraction

Slit Windows

Injector Faceplate

Replaceable Wall

Or 1"x1/2" Windows
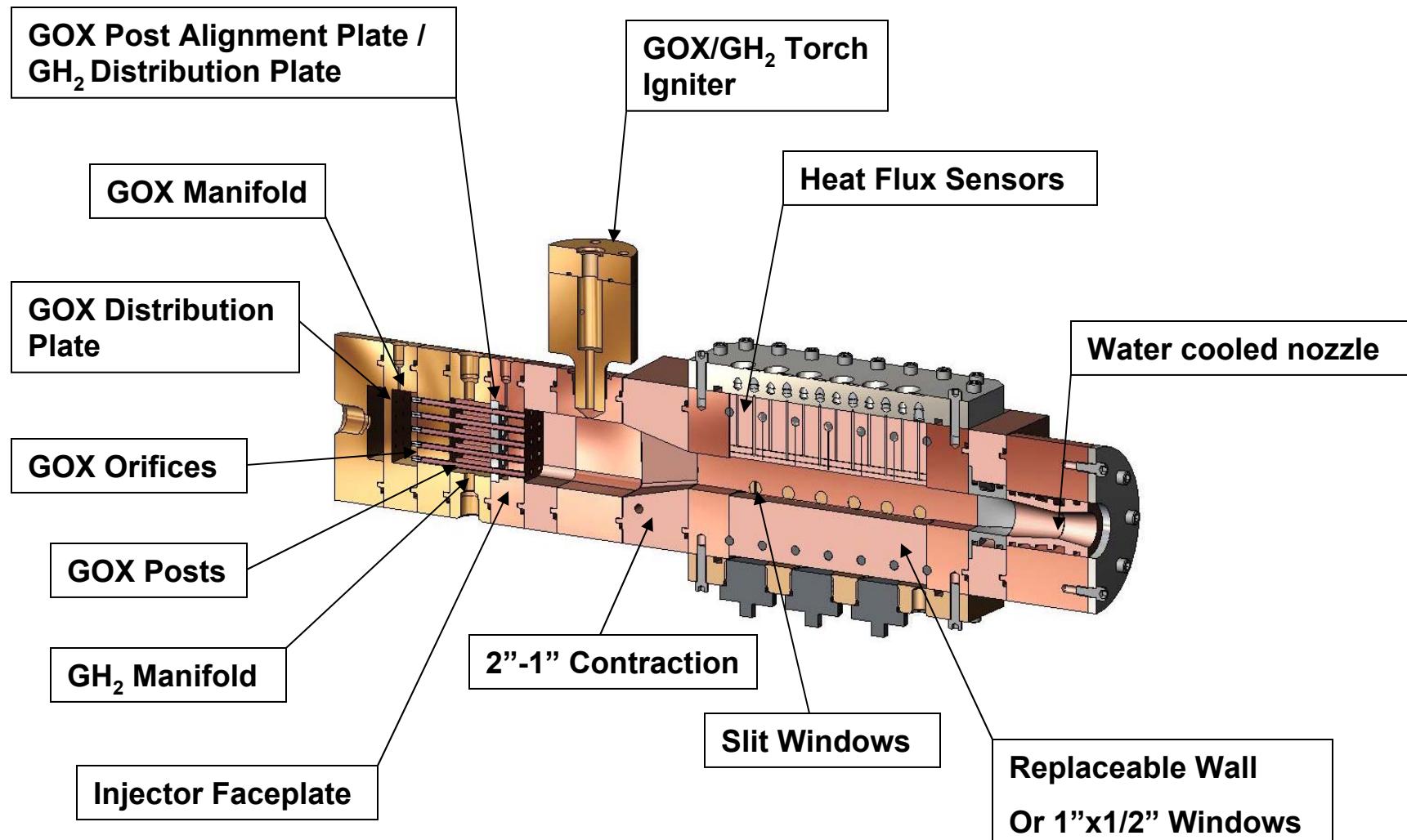
Heat Flux Sensor Requirements

- Operate at heat flux levels up to 50 MW/m2 (30 Btu/in2/s)

- Compatible with combustion products

- Can be inserted into a copper wall without disturbing the temperature or heat flux

- Response time of 0.1 seconds

- Measure heat flux to a wall with heat transfer enhancement features such as riblets or dimples

- Convenient to install and operate

Heat Flux Sensor Design

Polynomial Model

$$T_i = a + bx_i + cx_i^2 + dx_i^3$$

$$d = \frac{\dfrac{\dot{T}_2}{\alpha_2} - \dfrac{\dot{T}_1}{\alpha_1}}{6(x_2 - x_1)} \qquad c = \frac{\dfrac{\dot{T}_2}{\alpha_2}x_1 - \dfrac{\dot{T}_1}{\alpha_1}x_2}{2(x_1 - x_2)}$$

$$b = \frac{T_2 - T_1}{x_2 - x_1} - c\frac{x_2^2 - x_1^2}{x_2 - x_1} - d\frac{x_2^3 - x_1^3}{x_2 - x_1}$$

$$a = T_1 - b\,x_1 - c\,x_1^2 - d\,x_1^3$$

$$T_0 = a$$

$$q_0 = -k(T_0)\,b$$
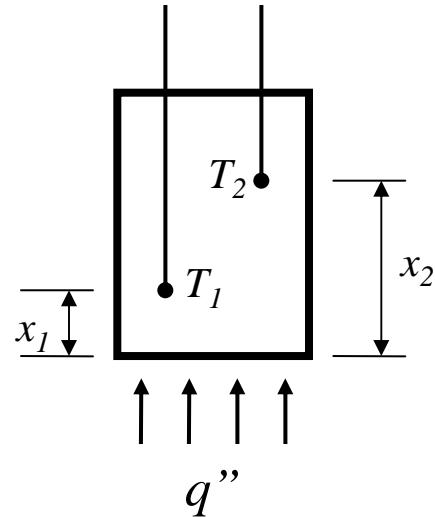
- **Eliminates surface junction thermocouple – improves survivability**

- **Embedded thermocouples are electrically "quiet"**

- **Compatible with ribs/dimples etc.**

Frequency Response of Sensor

Figure: Input heat flux (solid line) and Model heat flux (dotted markers), Heat Flux (normalized) vs Time (s), from 8.3 to 8.5 s.
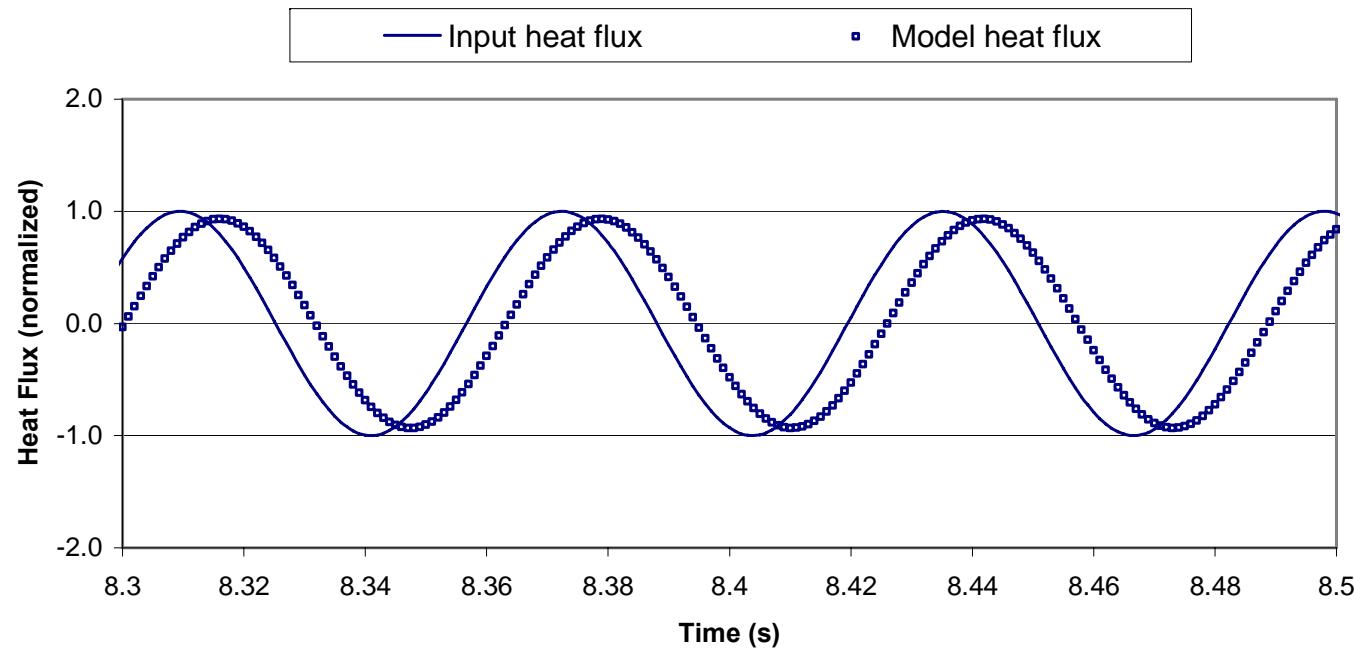
- **Response of sensor to 100 Hz sinusoidal heat flux input**
- **Copper, x_1=.075", x_2=.25", l=1.65"**

Bode Plot for Heat Flux
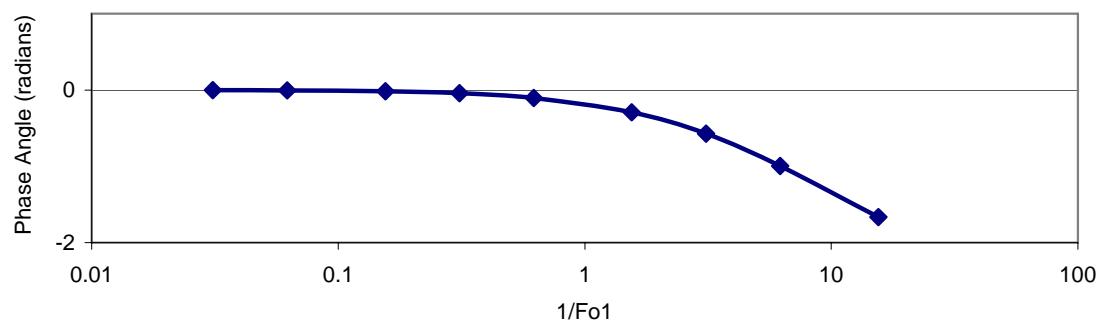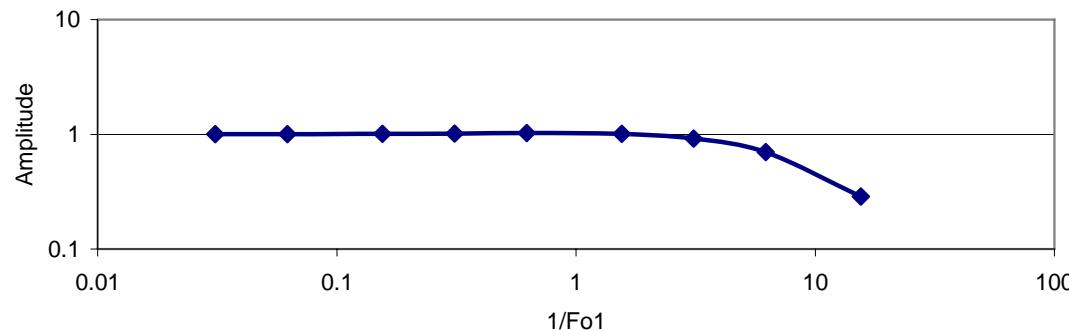
- **Assumes constant thermal properties (linear system)**
- **Amplitude and phase response plotted as function of reciprocal Fourier number, $1/Fo_1 = freq.\ x_1^2/\alpha$**
- **Negligible error below $Fo_1 = 1$**
- **same conditions as previous slide**

Bode Plot for Surface Temperature
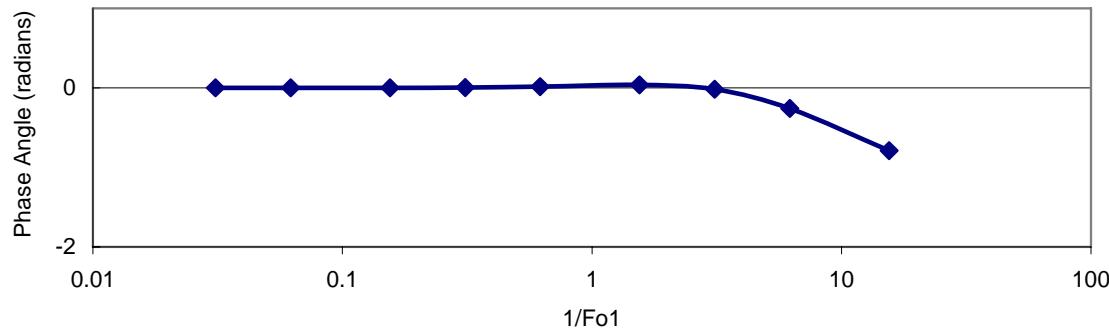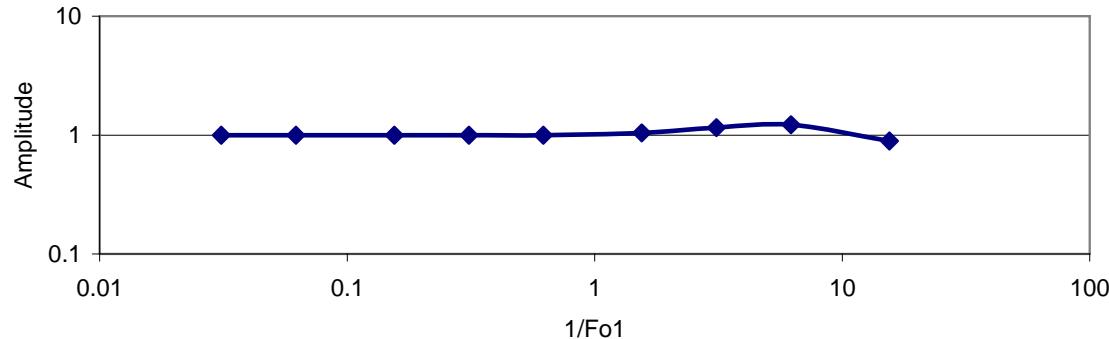
- Negligible error below $Fo_1 = 1$

- Same conditions as previous slide

Effect of Temperature Dependent Properties on Surface Temp.

- **Response to step change in heat flux to 3e7 W/m² at t=0**

- **Includes temperature dependent properties for copper**

- **After 0.1 s error is less than 0.1 K**

- **Problem modeled using MatLab pdepe (non-linear pde routine)**

**Distribution A: Public release, distribution unlimited**

16
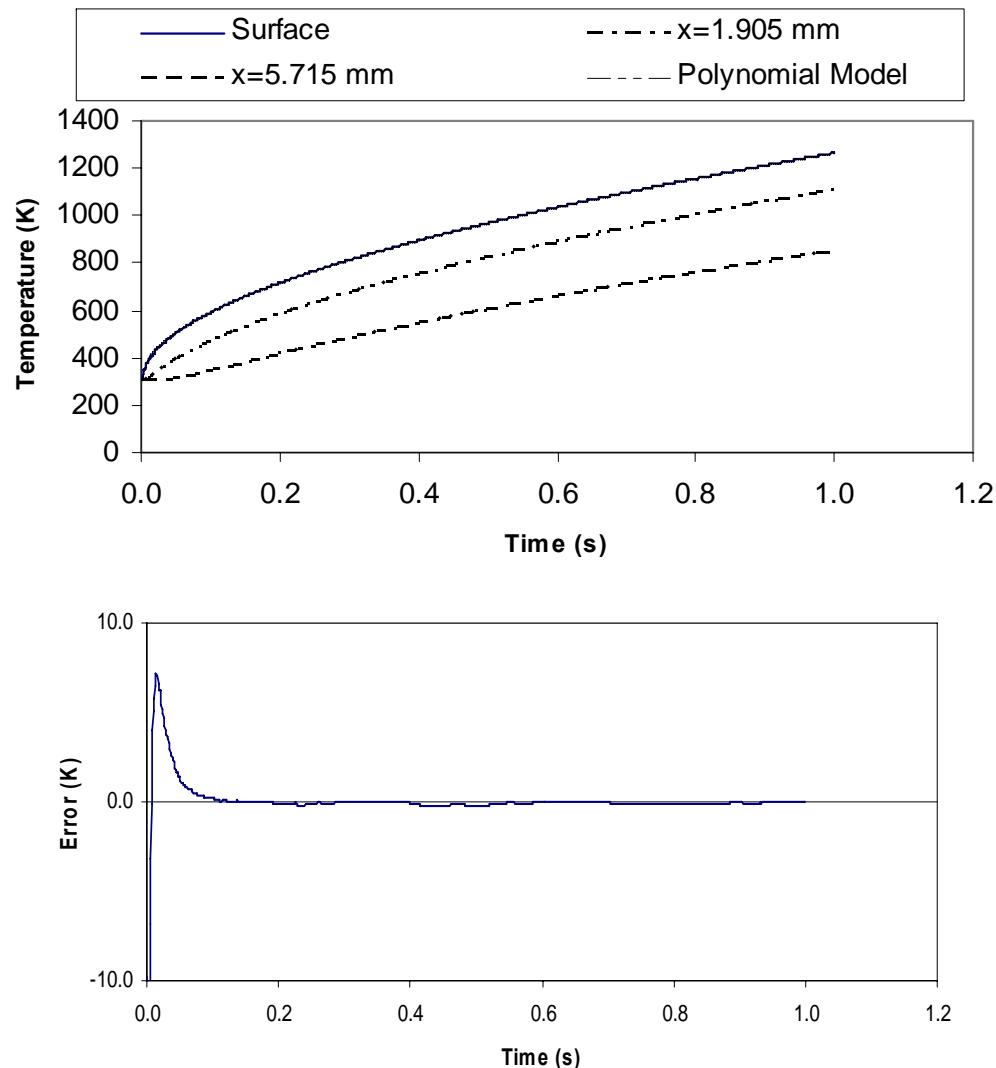
Effect of Temperature Dependent Properties on Heat Flux Prediction

- Same conditions as previous slide

- After 0.1 s heat flux error is less than 0.1%
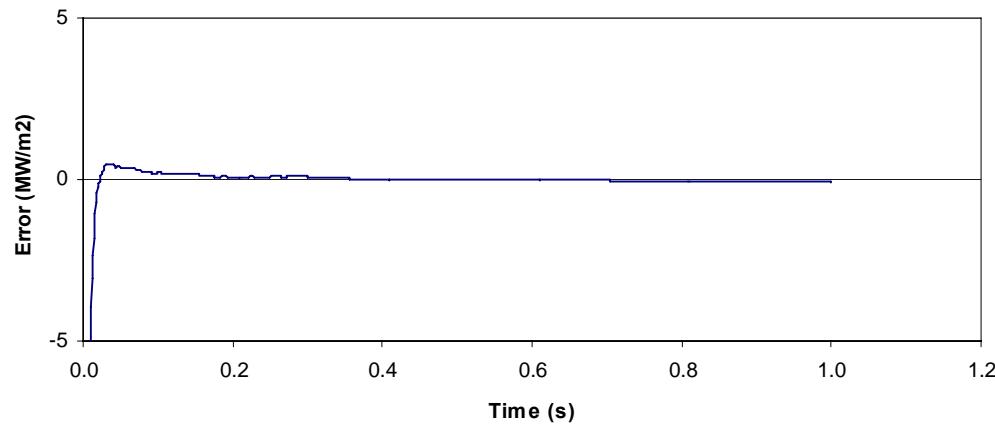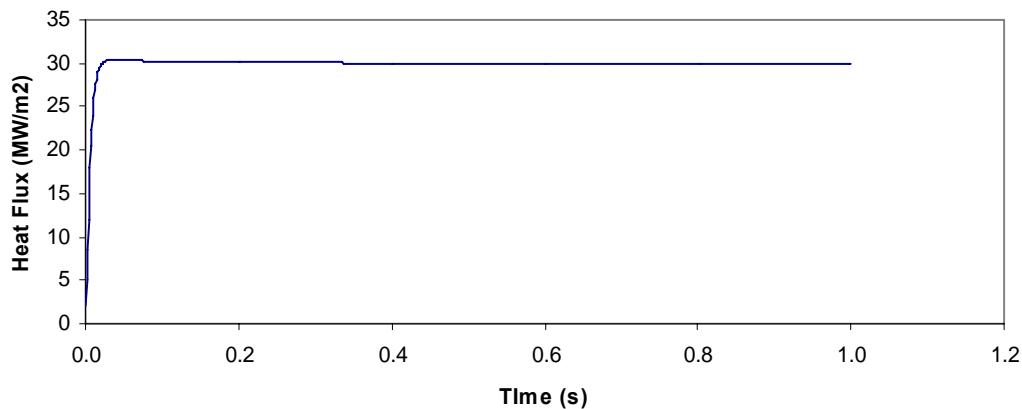
3-D Model of Heat Flux Sensor

t=0.1s   t=0.25s   t=0.5s   t=0.75s   t=1s
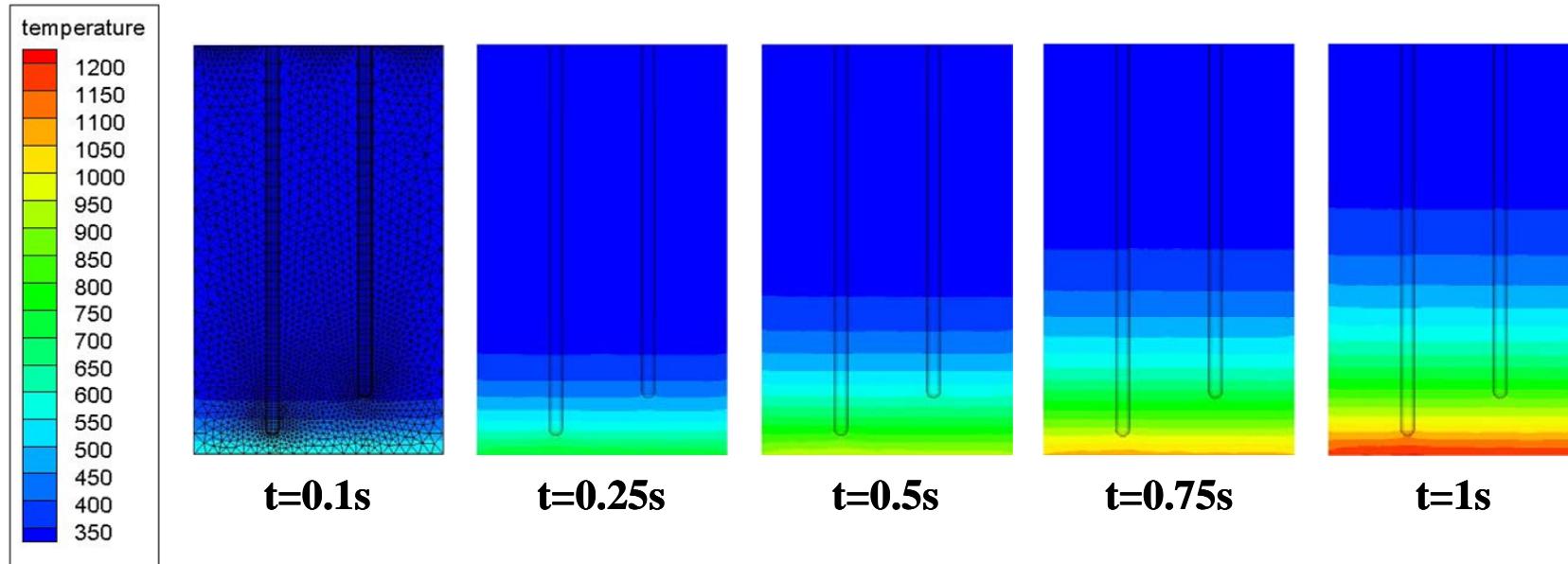
- **Thermocouples perturb flow of heat in sensor**
- **Thermocouple wells conservatively modeled as adiabatic wall**

# Effect of Thermocouples

• **Thermocouples cause error in heat flux prediction on order of 2%**

• **Error in surface temperture on order of 30 K. This would contribute about 1% error to Stanton number measurement.**
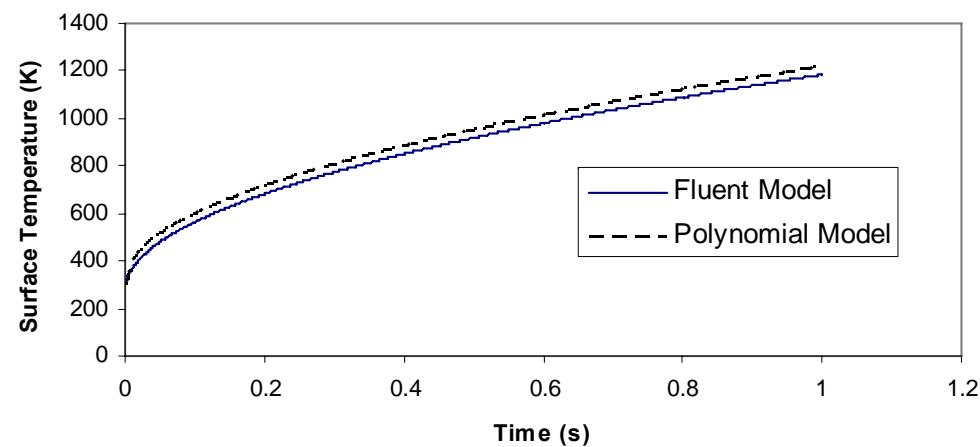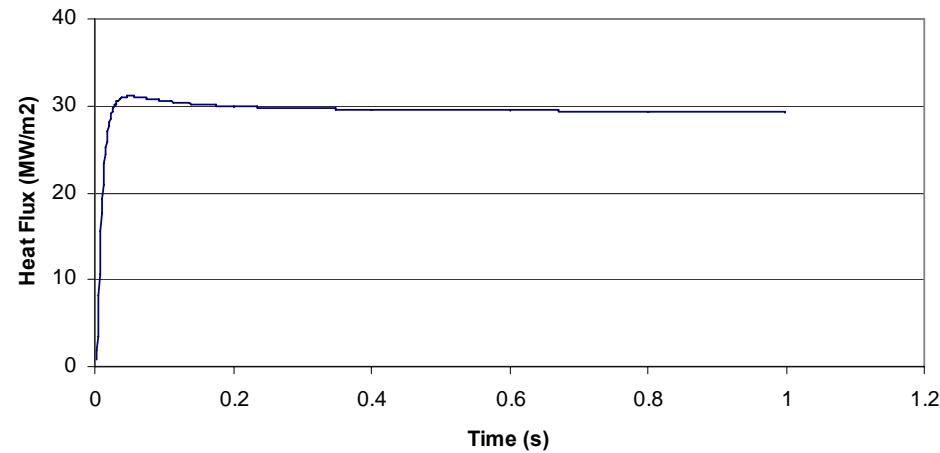
Heat Flux Block – In Process

1.65"

Grooves for TCs

Hole for alignment pin

Grooves for TC wire

After TC installation, halves are brazed with 80Cu/15Au/5P
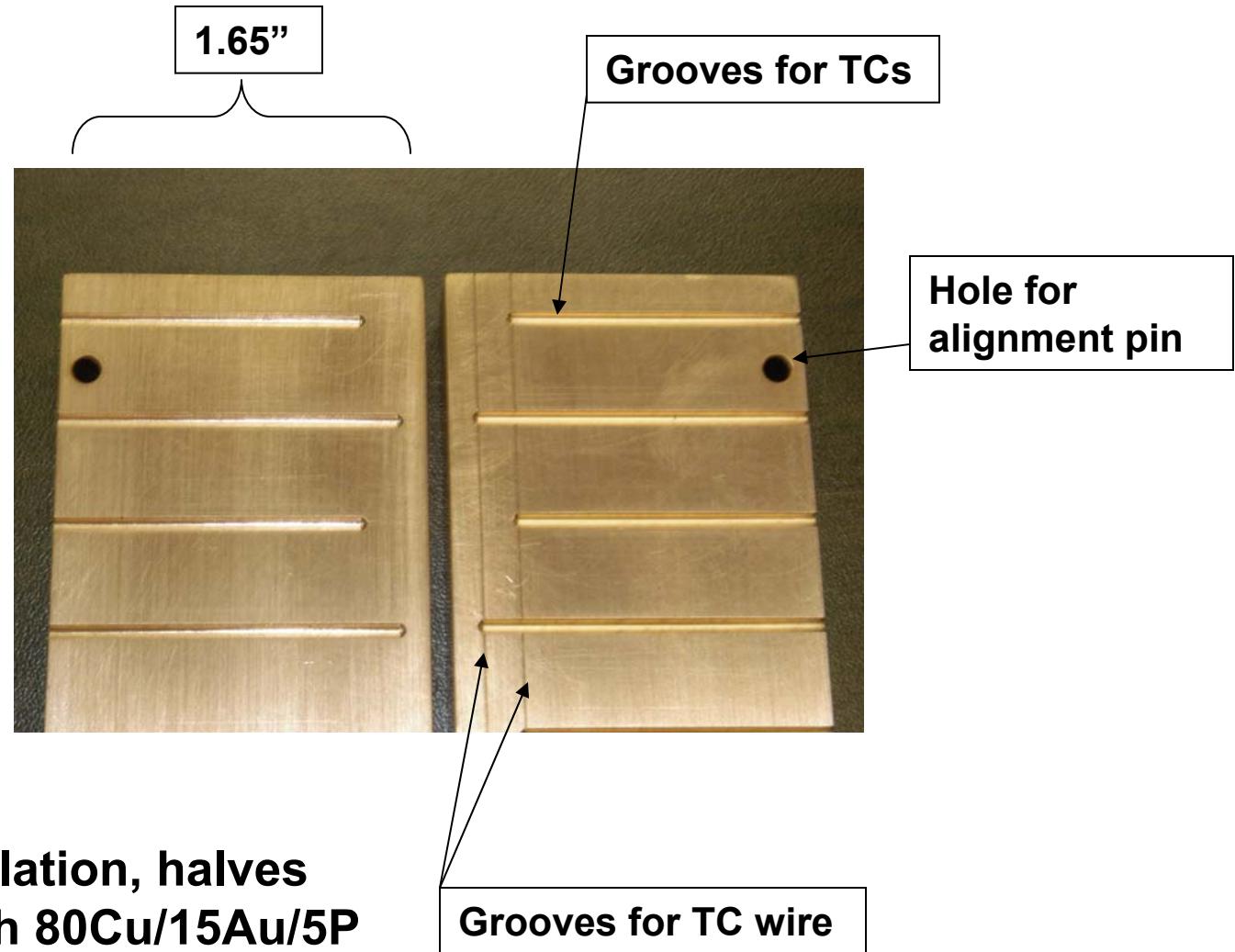
Thermocouple Installation

PRIOR TO BRAZING POT WITH OMEGA CC CEMENT OR EQUIVALENT

MUST MEET MINIMUM REQUIREMENT OF:

1. SERVICE TEMPERATURE OF 1400 F

2. RESISTANCE OF 1000 OHM/cm

NO POTTING COMPOUND IN INDICATED AREAS

ROLL EDGE OF T.C. WIRE CHANNEL OVER T.C. WIRE

T.C. WIRE

1. PRIOR TO INSTALLATION POT END OF T.C. SHEATH TO ENSURE THAT NO ELECTRICAL CONTACT EXIXT BETWEEN WIRES OR BETWEEN WIRES AND SHEATH. VERIFY THAT RESTANCE IS GREATER THAN 100K OHMS BETWEEN WIRES AND BETWEEN WIRES AND SHEATH.

2. POT IN PLACE AND ENSURE NO COTACT EXIST BETWEEN WIRES BY VISUAL INSPECTION.

3. VERIFY THAT RESISTANCE BETWEEN LEADS IS LESS THAN 5 OHMS

.125   .125

DETAIL A
SCALE 16 : 1

Distribution A: Public release, distribution unlimited

Conclusion

- **New heat flux rig is operational**

  – **Flexible design can serve as technology test bed for controlling chamber wall heat transfer**

  – **Careful control of flow enables rig to be used in CFD code validation studies**

- **New algorithm and sensor design provide reliable, accurate data on wall conditions**

- **Program is providing data on chamber wall heat transfer under conditions relevant to AF programs**

Backups

AFRL/PRSA EC-1 Facility

- EC-1 Facility in operation approximately 8 years
- 500 lbf thrust, 1250 psi chamber pressure
- Propellants: LHC, GH2, GCH4, GOX
- Highly operable, responsive facility
  - 10 tests/day typical
  - Can test nearly every day
  - Can quickly switch between test articles/fuels/conditions
- Personnel: 2 engineers, 2 mechanics
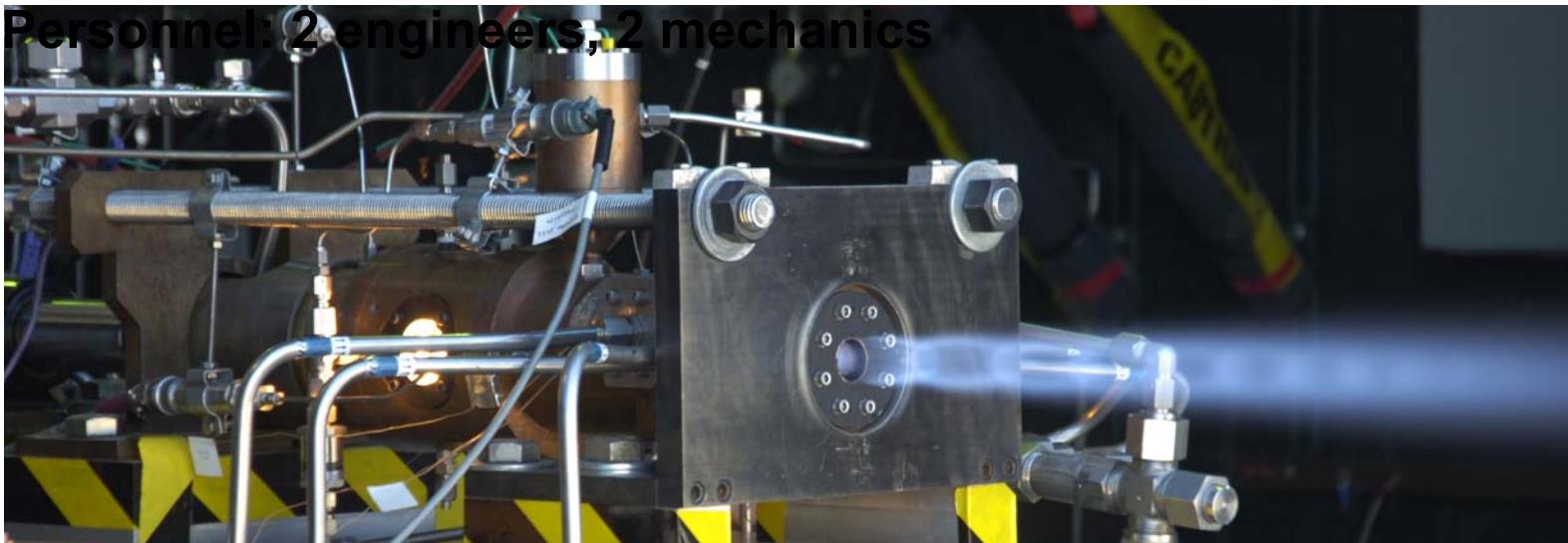
Stanton Number

Measurements:

Heat Flux: $\dot{T}_{CL}, T_{CL}, T_{OF_{-1}}, T_{OF_{+1}}$

$$k\,l\left(\frac{1}{\alpha}\dot{T}_{CL} - \frac{T_{OF_{-1}} - 2T_{CL} + T_{OF_{+1}}}{(\Delta y)^2}\right)$$

$$St = \frac{q''_W}{\rho_\infty U_\infty\,(h_\infty - h_W)}$$

Mass Flux: $\dot{m}_{O_2}, \dot{m}_{H_2}, A_C$

Gas Enthalpy: $P_C, \dot{m}_{O_2}, \dot{m}_{H_2}, A^*$

$$\left.\begin{array}{c} h_{ideal}(P_C, \dot{m}_{O_2}/\dot{m}_{H_2}) \\[1em] \eta_{C^*_{ideal}} = \dfrac{P_C A^*/(\dot{m}_{O_2} + \dot{m}_{H_2})}{C^*_{ideal}(\dot{m}_{O_2}, \dot{m}_{H_2}, A^*)} \end{array}\right\} \eta^2_{C^*}\,h_{ideal}$$

Wall Enthalpy: $T_{CL}, Fo = \alpha\,t/l^2$ $\qquad T_{Frontside}, P_C, \dot{m}_{O_2}/\dot{m}_{H_2}$

Heat Flux Model Validation Capabilities

Parameters that Influence Simulated Heat Flux	Current Measurement Method (q" Uncertainty Estimates)	Near-Term Uncertainty Estimates
Gas Temperature	ηC* & Equilibrium 6 %	IR Absorption / Emission Pyrometry 2 %
Surface Roughness	Comparison to Std. 5 %	Profilometer 1 %
Turbulence Intensity	N/A 4 %	LDV 1 %
Thermal Conductivity	Reference Data 1 %	same
O/F Mixture Ratio	Sonic Nozzles 2 %	Laser Induced Breakdown Spectroscopy 1%
Wall Temperature	Surface TC 0.5 %	same
Flow Acceleration	Calculation 0.5 %	same
Total Validation Uncertainty	± 9 %	± 3 %

Heat flux uncertainty estimates based on CFD Sensitivity Analysis

Distribution A: Public release, distribution unlimited

High Heat Flux Analysis

$T(x,t)$

q_{in}

x'
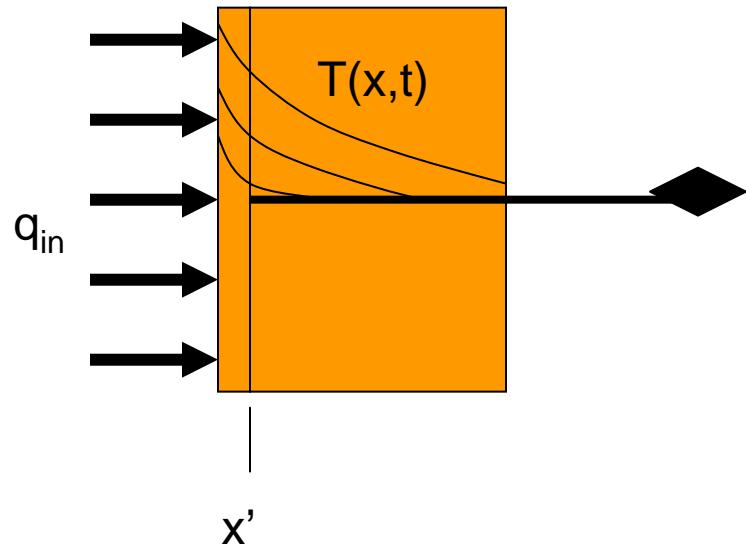
Data consist of time series $T(x',t)$
Solve for c_1 and c_2 from non-linear
Least squares fit to $T(x',t)$
Analytical solution assumes:
- semi-infinite slab
- initially uniform temperature in slab
- constant properties
- conduction is one-dimensional $\quad \dfrac{\partial T}{\partial x} >> \dfrac{\partial T}{\partial y}$

For $T(0,t)=c_1 t$

$$T_1(x,t) = c_1 t \left\{ \left(1 + \frac{x^2}{2\alpha t}\right) erfc\left(\frac{x}{2\sqrt{\alpha t}}\right) - \frac{x}{\sqrt{\pi \alpha t}} \exp\left(\frac{-x^2}{4\alpha t}\right) \right\}$$

For $T(0,t)=c_1 t^{1/2}$

$$T_2(x,t) = c_2 t^{1/2} \left\{ \exp\left(\frac{-x^2}{2\alpha t}\right) - \frac{x\sqrt{\pi}}{2\sqrt{\alpha t}} erfc\left(\frac{x}{2\sqrt{\alpha t}}\right) \right\}$$

By superposition

$$T(0,t) = T_0 + c_1 t + c_2 t^{1/2}$$

$$q(0,t) = -k \frac{\partial T(0,t)}{\partial x} = 2c_1 k \sqrt{\frac{t}{\pi \alpha}} + \frac{c_2 k}{2} \sqrt{\frac{\pi}{\alpha}}$$

Are Model Assumptions Valid?

- **Data obtained using a Medtherm coaxial TC**

- **Although both surface and backside temperture histories can be fit very accurately, they give significantly different results for heat flux.**

- **It appears that 1-D heat flow is not an accurate model**

Intercomparison of Inverse Heat Conduction Methods
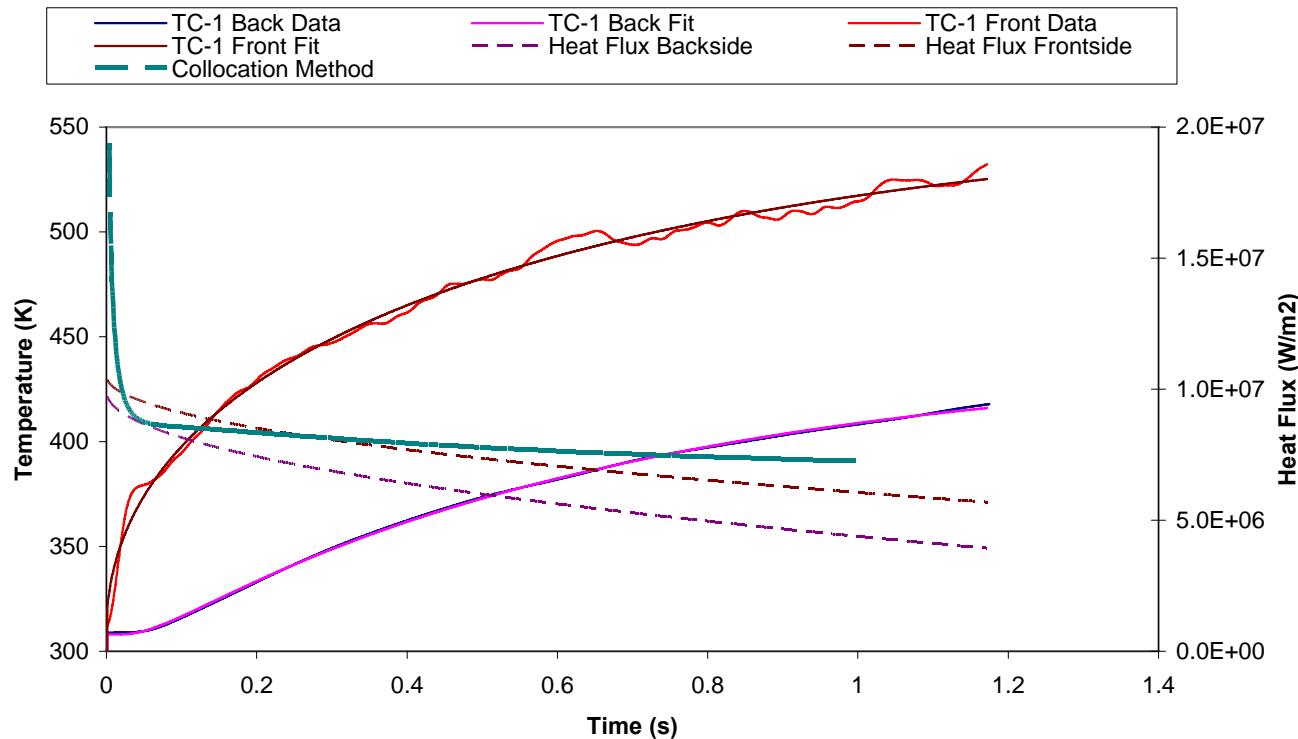
- **Data obtained with Medtherm Co-axial TC**

- **Significant deviations from 1-D theory indicates non-idealities in design**

It Only Gets Worse
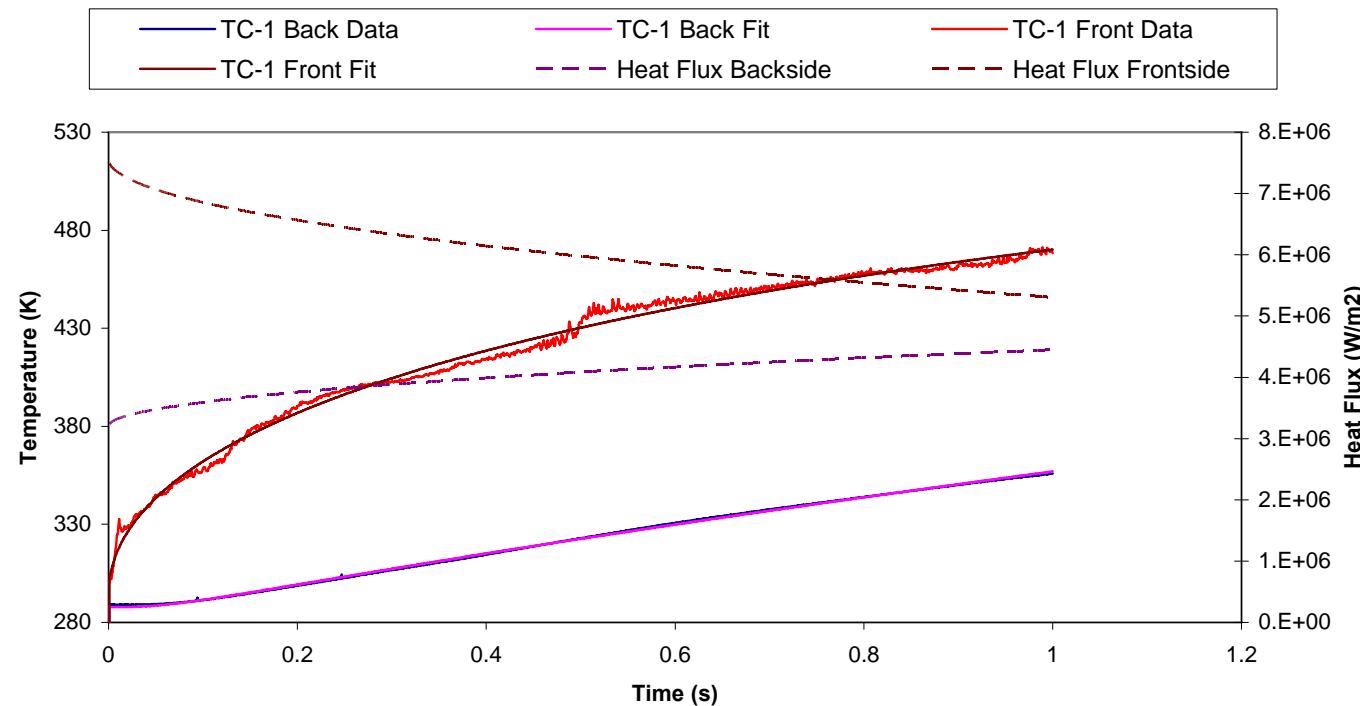
- **Front side is NANMAC eroding TC**

- **Backside is NANMAC in-wall TC**

- **Significant deviations from 1-D theory indicates non-idealities in design**

Transverse Conduction

- **Transverse conduction represents largest source of error in heat flux measurement, +/- 10% of total**

- **The variability may be due to real non-uniformities in the heat flux caused by hot-spots on the plate**

- **Best approach is probably a redesign of apparatus**

$$q_W '' = kl \left(\frac{1}{\alpha} \frac{\partial T}{\partial t} - \nabla^2 T \right)$$

Hot Spot?